Neutrophils activated by cancer cells and M2 macrophages promote gastric cancer progression during PD-1 antibody-based immunotherapy

Chenfei Zhou
Ruijin Hospital, Shanghai Jiao Tong University School of Medicine
Hui Yang
Ruijin Hospital, Shanghai Jiao Tong University School of Medicine
Liting Guo
Ruijin Hospital, Shanghai Jiao Tong University School of Medicine
Qu Cai
Ruijin Hospital, Shanghai Jiao Tong University School of Medicine
Wenqi Xi
Ruijin Hospital, Shanghai Jiao Tong University School of Medicine
Jing Liu
Ruijin Hospital, Shanghai Jiao Tong University School of Medicine
Fei Yuan
Ruijin Hospital, Shanghai Jiao Tong University School of Medicine
Huan Zhang
Ruijin Hospital, Shanghai Jiao Tong University School of Medicine
Chao Yan
Ruijin Hospital, Shanghai Jiao Tong University School of Medicine
Zhenggang Zhu
Ruijin Hospital, Shanghai Jiao Tong University School of Medicine
Jun Zhang
Ruijin Hospital, Shanghai Jiao Tong University School of Medicine
Lei Huang
Ruijin Hospital, Shanghai Jiao Tong University School of Medicine
Yan Shi (sy_rjh@aliyun.com)
Ruijin Hospital, Shanghai Jiao Tong University School of Medicine

---

Research Article

Keywords: Gastric cancer, neutrophil, immune checkpoint inhibitors, tumor microenvironment

Posted Date: April 19th, 2022

DOI: https://doi.org/10.21203/rs.3.rs-1556189/v1

Abstract

Biomarkers of immune checkpoint inhibitors (ICIs) in advanced gastric cancer (AGC) are under investigation. In present study, correlation between neutrophil-to-lymphocyte ratio (NLR) and efficacy of ICIs treatment in AGC patients as well as its underlying mechanisms were investigated based on clinical cases and single-cell RNA sequencing (scRNA-seq) analysis. NLRs early after treatment were correlated with disease progression and poor progression-free survival (PFS) of AGC patients. Neutrophil cluster1 (NE-C1) divided by scRNA-seq was the major cluster in peripheral blood samples and its proportion increased after PD-1 antibody treatment. NE-C1 had a neutrophil activation phenotype with high expression of *MMP9*, *S100A8*, *S100A9*, *PORK2*, and *TGF-β1.* Subclusters of malignant epithelial cells (EP-C4) and M2 macrophages (MF-C1, MF-C2) showed high neutrophil activating phenotypes. Strong interactions among NE-C1, EP-C4, MF-C1 and MF-C2 were identified. In summary, posttreatment NLR can be an early prognostic biomarker of AGC patients treated by PD-1 antibody-based therapy. Neutrophils activated by both tumor cells and M2 macrophages participate in promoting gastric cancer progression during PD-1 antibody-based treatment.

Introduction

HER2-negative advanced gastric cancer (AGC) patients treated by conventional chemotherapy have a miserable overall survival of less than 12 months due to limited therapeutic strategies options[1–3]. Immune checkpoint inhibitors (ICIs) have been approved to treat multiple malignant tumors, and now also become an effective option for AGC patients[4]. Firstly, ATTRACTION-2 and REGONIVO trials demonstrated the efficacy of nivolumab, or nivolumab plus regorafenib in chemotherapy-refractory late-stage gastric cancer patients, respectively[5, 6]. Recently, CHECKMATE-649 and ORIENT-16 trials demonstrated superior efficacy of PD-1 antibody plus chemotherapy comparing with chemotherapy along as first-line therapy for HER2-negative AGC patients[7, 8].

Although PD-1 antibodies have now been recommended in clinical practices to treat AGC patients based on these studies, overall response rate (ORR) of PD-1 antibody monotherapy in previous treated AGC patients is only about 10–20%. Some patients cannot benefit from PD-1 antibody-based therapy and even suffered a rapid disease progression[9]. A lot of biomarker investigations of ICIs, including tumor genome and neoantigen biomarkers, immune microenvironment phenotype, liquid biopsy and host-related markers, have been performed since its approvement and aim to identify patients who are more likely to response to the treatment[10]. For gastric cancer patients, combined positive score based on PD-L1 expression (CPS), microsatellite status and Epstein-Barr virus status are recommended to be assessed before ICIs treatment.

In addition to these biomarkers based on tumor tissue analysis, neutrophil-to-lymphocyte ratio (NLR) which is a mini-invasive, low-cost, and real-time method is now identified as a surrogate biomarker for ICIs treatment. The correlation between NLR and efficacy of ICIs treatment has been reported in several kinds of tumors, including lung cancer, renal cancer, and melanoma[11]. High NLR before or during

treatment indicated a poorer ORR and survival of ICIs treated patients[12]. Bi-directional regulation mechanism between tumor and host microenvironment play an important role in regulating tumor initiation and progression[13]. It can be inferred that the elevated neutrophil might directly participated in promoting tumor progression during ICIs treatment.

However, the correlation between NLR and efficacy of ICIs has not been verified in gastric cancer. Meanwhile, the underlying mechanisms of elevated NLR in promoting gastric cancer progression during ICIs treatment are also unclear. Therefore, we aimed to analyze the correlation between peripheral blood NLR and treatment efficacy of PD-1 antibody-based therapy in a cohort of AGC patients. Single-cell RNA sequencing (scRNA-seq) was performed on samples that were obtained from AGC patients before and after ICIs treatment to understand the underlying molecular mechanisms.

Materials And Methods

Patients and samples

Clinicopathological information of 68 gastric cancer patients who underwent systemic therapy from July 2020 to December 2022 in Department of Oncology, Ruijin Hospital were collected retrospectively. All patients were pathologically confirmed as gastric adenocarcinoma with metastatic diseases. Patients were treated by PD-1 antibody-based therapy, including monotherapy, chemotherapy combined, and anti-angiogenesis inhibitor combined. Efficacy endpoints including objective response rate (ORR) and progression-free survival (PFS) were recorded. NLR at time of baseline (BL), second cycle (2C) and first imaging assessment of efficacy (usually at 9-week, AE1) was retrieved and calculated based on results of patients' blood routine tests.

For scRNA-seq, multiple samples from 2 patients in this cohort before and after treatment were obtained, including stomach primary lesions, peripheral blood samples and pleuroperitoneal fluids. Written informed consent were provided before biopsy. The protocol was approved by ethics committee of Ruijin Hospital, Shanghai Jiao Tong University School of Medicine, Shanghai, People's Republic of China.

Tissue dissociation and preparation

The fresh tumor tissue was stored in the sCeLiVE^{TM} Tissue Preservation Solution (Singleron) and all the samples were transported to the Singleron lab at a temperature of 2°C to 8°C. The specimens were washed with Hanks Balanced Salt Solution (HBSS) for 3 times and minced into 1–2 mm pieces. Then the tissue pieces were digested with 2ml sCeLiVE^{TM} Tissue Dissociation Solution (Singleron) at 37℃ for 15min in 15ml centrifuge tube with sustained agitation. After digestion, using 40-micron sterile strainers to filter the samples and centrifuging the samples at 1,000 rpm for 5 minutes. Then the supernatant was discarded, and the sediment was resuspended in 1ml PBS (HyClone). The PBMCs were isolated by density gradient centrifugation using Ficoll-Paque Plus medium (GE Healthcare) and washed with Ca/Mg-free PBS. To remove the red blood cells, 2 mL GEXSCOPE^{TM} red blood cell lysis buffer (Singleron)

was added at 25°C for 10 minutes. The solution was then centrifuged at 500 × g for 5 min and suspended in PBS. The blood samples were centrifuged at 400g for 5 min at 4°C, and the supernatant was discarded. After removed red blood cells, PBMCs were isolated by centrifuged at 400g for 10min at 4°C. The supernatant was discarded and the PBMCs were resuspended by phosphate buffered saline to obtain a single-cell suspension. The sample was stained with trypan blue (Sigma) and microscopically evaluated.

Single cell RNA sequencing

Single-cell suspensions with 1×10^5 cells/mL in concentration in PBS (HyClone) were prepared. Single-cell suspensions were then loaded onto microfluidic devices and scRNA-seq libraries were constructed according to Singleron GEXSCOPE^R protocol by GEXSCOPE^R Single-Cell RNA Library Kit (Singleron Biotechnologies)[14]. Individual libraries were diluted to 4nM and pooled for sequencing. Pools were sequenced on Illumina HiSeq X with 150 bp paired end reads.

Primary analysis of raw read data

Raw reads were processed with fastQC and fastp to remove low quality reads. Poly-A tails and adaptor sequences were removed by cutadapt. After quality control, reads were mapped to the reference genome GRCh38 (Ensembl version 92 annotation) using STAR. Gene counts and UMI counts were acquired by featureCounts software[15]. Expression matrix files for subsequent analyses were generated based on gene counts and UMI counts.

Quality control, dimension-reduction and clustering

Cells were filtered by gene counts between 200 to 5,000 and UMI counts below 30,000. Cells with over 50% mitochondrial content were removed. After filtering, 80,680 cells were retained for the downstream analyses, with on average 832 genes and 2,356 UMIs per cell. We used functions from Seurat v3.1.2 for dimension-reduction and clustering[16]. All gene expression was normalized and scaled using NormalizeData and ScaleData. Top 2000 variable genes were selected by FindVariableFeautres for PCA analysis. Cells were separated into 37 clusters by FindClusters, using the top 20 principal components and resolution parameter at 1.2. For subclustering of epithelial cells, macrophages, M2 macrophages, and neutrophils, we set the resolution at 0.3, 0.5, 0.3, and 1.2, respectively. UMAP (Uniform manifold approximation and projection) algorithm was applied to visualize cells in a two-dimensional space. Harmony v1.0 be used to integrate samples and performed downstream analysis.

Differentially expressed genes (DEGs) analysis

Genes expressed in more than 10% of the cells in a cluster and with average log (Fold Change) of greater than 0.25 were selected as DEGs by Seurat v3.1.2 FindMarkers based on Wilcox likelihood-ratio test with default parameters.

Cell type annotation

The cell type identity of each cluster was determined with the expression of canonical markers found in the DEGs using SynEcoSysR database. Heatmaps displaying the expression of markers used to identify each cell type were generated by Seurat v3.1.2 DoHeatmap.

Pathway enrichment analysis

To investigate the potential functions of cellular subclusters, the Gene Ontology (GO) and Kyoto Encyclopedia of Genes and Genomes (KEGG) analysis were used with the “clusterProfiler” R package 3.16.1[17]. Pathways with p_adj value less than 0.05 were considered as significantly enriched. Gene Ontology gene sets including molecular function (MF), biological process (BP), and cellular component (CC) categories were used as reference.

scRNA-seq based CNV detection

The InferCNV package was used to detect the CNVs in subclusters of epithelial malignant cells. Immune non-malignant cells were used as baselines to estimate the CNVs of malignant cells. Genes expressed in more than 20 cells were sorted based on their loci on each chromosome. The relative expression values were centered to 1, using 1.5 standard deviation from the residual-normalized expression values as the ceiling. A slide window size of 101 genes was used to smoothen the relative expression on each chromosome, to remove the effect of gene-specific expression.

Cell-cell interaction analysis

CellCall v0.0.0.9000 was used to analyze the intercellular interaction based on the receptor-ligand interaction between two cellular clusters and inferred the signaling pathways of the internal regulation[18]. The fraction of ligand-receptor genes interactions between cellular clusters was assessed by integrating the L2 norm of the receptor-ligand interaction and the activity fraction of downstream TFs, which was calculated by the inbuilt GSEA algorithm. Finally, Ligand-receptor-TFs with a significant interaction between cellular clusters was selected by using hypergeometric test and a p-value less than 0.05. Visualization was performed by using the inbuilt plotting functions from CellCall.

Statistical analysis

Correlation of NLR with clinicopathological characteristics and treatment response of gastric cancer was analyzed by one-way ANOVA test. Log-rank test in Kaplan-Meier method and Cox proportional hazards model were used to analyze prognostic factors. *P*-value<0.05 was considered as statistically significant. All tests were performed by SPSS 22.0 software (SPSS Inc.).

Results

High NLR after PD-1 antibody treatment indicated poor efficiency of AGC patients

The clinical information of 68 AGC patients (46 males and 22 females) was listed in Table 1. Nearly 78% patients treated with PD-1 antibody-based therapy as the second-line or more. Most patients received combination therapeutics. Median number of treatment cycles were 5 (2-26). Median NLR at BL, 2C and AE1 were 3.74, 2.91 and 3.28, respectively. No significant difference of NLR at three timepoints was found among patients with different metastatic organs, pervious lines of treatment and combination strategies.

NLR-AE1 was significantly different among patients with different objective response (PD vs. SD, 7.29±6.80 vs. 3.64±2.58, *P*=0.003; PD vs. PR, 7.29±6.80 vs. 2.92±1.24, *P*=0.013, Figure 1A). NLR-2C of PD patients was also higher than SD patients (4.76±2.83 vs. 3.26±2.71, *P*=0.037), while no significant different was identified comparing with PR patients (4.76±2.83 vs. 3.43±1.22, *P*=0.203, Fig. 1B). Correlation between NLR-BL and patients' ORR was not identified (Fig. 1C).

Median PFS of all patients was 3.5 months (0.4 to 30.1 months). The 75th percentile of NLR was selected as the cut-off value to distinguish high and low NLR (NLR-2C=4.83; NLR-AE1=5.12). Kaplan-Meier analysis showed that patients with high NLR-2C had poorer PFS comparing with those with low NLR-2C (6.4m vs. 3.0m, *P*=0.025, Fig. 1D), as well as for patients with high NLR-AE1 (9.4m vs. 2.4mm, *P*=0.008, Fig. 1E). Multivariable analysis showed that high NLR-AE1 was the independent prognostic factor for those patients (HR=2.47, 95%CI 1.25-4.90, *P*=0.01).

Multiple samples analysis by scRNA-seq in patients treated by PD-1 antibody

Multiple samples from two treatment refractory AGC patients in this cohort were analyzed by scRNA-seq. PD-1 antibody plus anti-angiogenesis inhibitor was administrated for both patients. Patient 1 (P1) was a young female with hepatic and pleural metastases. Before treatment, samples from stomach primary lesion, peripheral blood, pleural and ascitic fluid were obtained. After 1 cycle of treatment, performance status of P1 deteriorated too rapidly to receive second cycle due to disease progression, then pleural fluid and peripheral blood samples were re-collected, and best support care was given afterward (Fig. 2A). Patient 2 (P2) was also a female with peritoneal metastasis. Samples from stomach primary lesion, peripheral blood and ascitic fluid were collected before and after treatment. The patient stopped treatment due to bowel obstruction caused by peritoneal metastasis, and no significant disease progression was observed at that time (Fig. 2B).

Total 80,680 cells from 12 samples were obtained, detail number of cells in each sample was showed in Table S1. UMAP algorithm was performed to visualize cell clusters (Fig. 2C). Major cell clusters including endothelial cells (ECs), epithelial cells, myeloid cells, myofibroblasts, pleural mesothelial cells (PMCs), pericytes, plasma cells, platelets, T cells, plasmacytoid dendritic cells (pDCs) and B cells were annotated by established marker genes (Fig. 2D, Fig S1).

Subcluster of neutrophil with activation phenotype accounted for major proportion in peripheral blood samples

Peripheral blood samples before and after treatment were analyzed first. Myeloid cells and T cells accounted for the major parts of all four samples. Proportion of myeloid cells increased while T cells decreased after treatment. The proportion of neutrophil which was a major part of myeloid cells significantly increased after treatment in both patients (Fig. 3A). Then, neutrophils in peripheral blood samples and ascites were divided into 7 cellular subclusters. The constitution of neutrophil subclusters between peripheral blood samples and ascites was different. Neutrophil cluster1 (NE-C1) dominated in peripheral blood samples (Fig. 3B).

GO enrichment analysis of biological function based on high-expression DEGs of NE-C1 showed that those DEGs were mainly enriched in neutrophil activation phenotype. The top 3 biological functions included neutrophil activation, neutrophil activation involved in immune response, and neutrophil degranulation (Fig. 3C). Furthermore, cancer-promoting genes including *MMP9*, *S100A8*, *S100A9*, *PORK2*, *TGF-β1* were identified as high-expression DEGs in NE-C1 (Fig. 3D).

Subclusters of malignant epithelial cells participated in regulating neutrophil activation

Malignant epithelial cells were identified by inferred CNV algorithm. Those cells could be found in primary lesion and pleural fluid of P1, and primary lesions of P2. Then, malignant epithelial cells were divided into 13 cellular subclusters (Fig. 4A). Distribution of subclusters in P1 and P2 was significantly different, while epithelial cell cluster 4 (EP-C4) could be found in both patients, especially as a new cluster for P2 after treatment (Fig. 4B).

GO enrichment analysis of biological function showed that high-expression DEGs in EP-C4 were mainly enriched in neutrophil activation, neutrophil mediated immunity, and neutrophil degranulation. Cell-cell junction organization and cell-matrix adhesion were also enriched (Fig. 4C). KEGG enrichment analysis showed that high-expression DEGs in EP-C4 were enriched in leukocyte trans-endothelial migration pathway, as well as in regulation of actin cytoskeleton and focal adhesion pathways (Fig. 4D).

Subcluster of M2 macrophage participated in regulating neutrophil activation

In all non-peripheral blood samples, myeloid cells had high proportion after malignant epithelial cells, and could be divided into macrophage, monocytes, dendritic cells, and neutrophils (Fig. S2). Macrophage polarization was reported participated in modulating tumor immune microenvironment. Therefore, macrophages were further classified as M1 and M2- macrophages, in which M2 macrophages accounted for a major part (Fig. 5A). Eight cellular subclusters of M2 macrophage were subdivided. M2 macrophage cluster1 (MF-C1) was only found in samples of P1, while MF-C2 was found in both patients and mainly in primary lesions (Fig. 5B).

GO enrichment analysis showed that high-expression DEGs of MF-C1 were mainly enriched in neutrophil activation, neutrophil degranulation, and neutrophil activation involved in immune response (Fig.5C). Meanwhile, high-expression DEGs of MF-C2 could also be enriched in regulation of leukocyte differentiation and positive regulation of leukocyte activation (Fig.5D).

Cellular interaction among neutrophil, M2 macrophage and tumor cell attributed to tumor progression during PD-1 antibody treatment

Cellular interaction among all cellular subclusters of neutrophil, M2 macrophage and malignant epithelial cell were illustrated by heatmap of paired ligands and receptors (pLRs) (Fig. 6A). For P1, EP-C3, EP-C4, EP-C6 and EP-C9 were found that had a high number of pLRs with both M2 macrophage and neutrophil. A high number of pLRs was also found among different cellular subclusters of M2 macrophage and neutrophils. For P2, EP-C4 and EP-C7 were found that had a high number of pLRs with M2 macrophage and neutrophil. MF-C2 had highest number of pLRs with all subclusters of neutrophil.

Interactions among NE-C1, EP-C4, MF-C1 and MF-C2 were further analyzed. Receptor-ligand interactions among those cellular subclusters showed that MF-C2 could provide ligands for both NE-C1 and EP-C4, while ligands of MF-C1 could only interact with receptors of NE-C1. Bi-directional interaction between NE-C1 and EP-C4 was identified (Fig. 6B).

Detail pLRs between different cellular subclusters were analyzed by communication score heatmap. Between NE-C1 and EP-C4, ligand-receptor interactions including *OSM-OSMR*, *IL1B-IL1RAP*, *OSM-IL6ST* and *TGFB1-TGFBR2* were identified, and *SERPINF1-LRP6*, *HGF-EPHA2*, *IGF1-INSR*, *HGF-ERBB2* and *HGF-MET* were found between MF-C2 and EP-C4. Chemokines and their receptors were identified as major interactions of MF-C1/NE-C1, MF-C2/NE-C1 and EP-C4/NE-C1. KEGG enrichment analysis showed that ligand-receptor interactions between NE-C1 and EP-C4 were enriched in MAPK signaling pathway and Jak-STAT signaling pathway. For MF-C2 and EP-C4, PI3K-Akt signaling pathway was identified. Chemokines signaling pathway was identified between MF-C1/NE-C1, MF-C2/NE-C1 and EP-C4/NE-C1 (Fig. 6C).

Discussion

In present study, to assess the prognostic value of elevated NLR in AGC patients treated by PD-1 antibody-based therapy, clinical information of AGC patients was reviewed and analyzed first. Then, scRNA-seq analysis was performed based on pre- and posttreatment samples to further explore the underlying mechanisms of elevated NLR during tumor progression. By scRNA-seq analysis, close interactions among neutrophil, M2 macrophage and tumor cells were identified, which indicated a positive feedback loop between tumor and host microenvironment playing an important role in tumor progression during ICI treatment (Fig. 7).

Prognostic value of NLR was identified in multiple kinds of tumors. In gastric cancer, Sun et al. reviewed 19 studies including 5421 patients with different stages who were treated by chemotherapy and/or surgical resection showed that elevated pretreatment NLR was a negative prognostic biomarker for patients' outcome[19]. For ICIs treatment, the value of NLR as a prognostic biomarker in gastric cancer is uncertain. Seventy-one gastric cancer patients were enrolled in a pan-cancer investigation which assessed the correlation between pretreatment NLR and efficacy of ICIs treatment. Confidence interval of

hazard ration of pretreatment NLR crossed 1.0 for gastric cancer subgroup[12]. Based on current cohort, posttreatment NLR were found had significant correlation with ORR and PFS of AGC patients treated by PD-1 antibody-based therapy, and NLR at first imaging assessment of efficacy was identified as an independent prognostic factor.

Timepoints of NLR assessed among previous studies were different, while both pre- and posttreatment NLR was reported to associate with patients' prognosis. For metastatic renal cell carcinoma, NLR at 6 weeks was indicated as a significantly stronger predictor comparing with NLR at baseline[20]. Pretreatment NLR was associated with outcome of lung cancer and melanoma treated by ICIs[21, 22]. This heterogenous phenomenon may attribute to the different sample size, tumor types, and therapeutics of those studies. Our study firstly reported the prognostic value of posttreatment NLR during PD-1 antibody-based treatment for gastric cancer patients, which could be used as a convenient method to predictive outcome and monitor the efficacy of treatment.

The role of neutrophils during progression of ICIs treatment of gastric cancer was barely investigated. Functions of neutrophil in tumor initiation and progression have been recognized in the past few years, which can promote malignant behaviors of tumor cells by producing reactive oxygen species, cytokine, proteinase, and angiogenesis factors[23, 24]. In present study, a subcluster of neutrophil with activation phenotype accounted for a significant proportion of PB samples before and after treatment, which also highly expressed well-known tumor promoting genes including *MMP9*, *S100A8*, *S100A9*, *PORK2*, and *TGF-β1*. Therefore, we presumed that this subcluster of neutrophil could be one of the stimuluses of tumor progression during PD-1 antibody treatment and accounted for elevated NLR as negative prognostic biomarker.

Recruitment and activation of neutrophils can be induced by tumor cells in cancer patients[23, 25]. EP-C4, a common subcluster of malignant epithelial cells in both patients, displayed a high neutrophil activating phenotype, which indicated that it may attribute to the elevated NLR during PD-1 antibody treatment. However, PD-1 antibodies mainly target on immune cells infiltrated in tumor microenvironment[26]. Tumor-infiltrating $CD8^+$ T cell which is the major therapeutic target of PD-1 antibodies could not be found in non-peripheral blood samples of our two patients (Fig. S1). In addition to T cells, myeloid cells including dendritic cells and macrophages can be found in tumor microenvironment interacting with PD-1 antibody[27, 28]. It has been reported that M2 macrophages infiltration is a negative factor which can impair treatment efficacy of PD-1 antibody[29]. In present study, M2 macrophages accounted for a significant proportion of tumor infiltrated immune cells. Two cellular subclusters of M2 macrophage with neutrophil activating phenotype were identified which could attributed to the elevated NLR after treatment.

The interaction between tumor cells and tumor microenvironment play an important role in tumor progression and treatment resistance. We found that both tumor cells and M2 macrophages had the capability to activate neutrophil. Meanwhile, neutrophil subcluster with high activation could result in

tumor progression. Therefore, cell-cell interaction among tumor cells, neutrophils and macrophages was further analyzed. Close interactions were found among those cells. NE-C1 could regulate the activation of Jak-STAT and MAPK signaling pathways in EP-C4, which were both tumor-promoting pathways. Moreover, it was reported that activation of Jak-STAT pathway in tumor cells after PD-1 antibody treatment could stimulate MDM2 expression and induce treatment resistance[30]. Both subclusters of M2 macrophages could regulated NE-C1 through chemokine signaling pathway, and MF-C2 could also regulated PI3K-Akt signaling pathway of EP-C4 which was also a well-known tumor-promoting pathway. Although direct interaction between MF-C1 and EP-C4 was not identified, it might also participate in tumor progression indirectly by modify activation of NE-C1.

The communication score heatmap showed that *HGF* which was one of the important oncologic molecular of gastric cancer was identified as the major ligand of MF-C2. Targeting HGF/c-Met pathway combining with chemotherapy has been trialed in AGC patients as first-line therapy. However, the result was not promising[31, 32]. Its combination with PD-1 antibody has not been investigated currently. Our results indicated that anti-HGF could be a potential combination strategy to enhance the efficacy of ICIs treatment of gastric cancer by interfering the interaction between M2 macrophage and tumor cells. On the other hand, *OSM* and *IL1B* provided by NE-C1 were found participated in regulating Jak-STAT signaling pathway and MAPK signaling pathway of EP-C4. *OSM* was found participated in regulating malignant behaviors of multiple tumors including gastric cancer[33]. Further works should be performed to understand their role during PD-1 antibody treatment and facilitate developing potent combination therapy.

By the results of cellular interaction analysis, macrophage seemed to be identified as a critical regulator of tumor progression and host inflammation status which could regulate both tumor cells and neutrophil. It was reported that PD-1 antibody could be captured by PD-1 negative macrophages through its interaction with Fcγ receptor of macrophages[34, 35]. This interaction could impair anti-tumor activity of PD-1 antibody though reprogramming tumor associated macrophage (TAM)[36]. For MF-C1, *FCGR3A* and *FCGR2B* were identified as high-expression DEGs. Fcγ receptors encoded by *FCGR3A* and *FCGR2B* could interact with Fc fragment of PD-1 antibody[37] and might result in tumor-promoting phenotype of macrophages during treatment. Therefore, we presumed that M2 macrophage reprogrammed by PD-1 antibody could drive tumor progression by triggering cellular interaction between tumor and immune cells. However, this hypothesis should be verified based on clinical samples.

Conclusion

Posttreatment NLR could be an early prognostic biomarker of AGC patients who were treated by PD-1 antibody-based therapy. Activation of neutrophil was induced by both tumor cells and M2 macrophages, in return, neutrophil and M2 macrophage could regulate critical tumor-promoting pathways. This positive feedback loop could attribute to tumor progression after PD-1 antibody treatment of AGC patients,

Declarations

Acknowledgments

We thank staff of Singleron Co. for assistance of samples analysis and data processing.

Funding

The study was supported by National Natural Science Foundation of China (81802319, 81900146); Shanghai Municipal Health Bureau Project (No.2020CXJQ03); and GUANGCI Distinguished Yong Scholars Training Program, 2019 (GCQN-2019-A10).

Competing interests

The authors have declared that no competing interest exists.

Author contributions

The study conceived and designed by Chenfei Zhou, Yan Shi and Lei Huang. Experiments and data analysis were performed by Chenfei Zhou, Hui Yang, Liting Guo and Qu Cai. Sample collection was performed by Liting Guo and Chao Yan. Pathological diagnosis was performed by Fei Yuan. Radiological diagnosis and efficacy assessment was performed by Huan Zhang. The manuscript was written by Chenfei Zhou and Hui Yang. The study was supervised by Jun Zhang and Zhenggang Zhu. All authors read and approved the final manuscript.

Data availability

The authors confirm that the data supporting the findings of this study are available within the article and its supplementary materials. The datasets generated during current study are available from the corresponding author on reasonable request.

Ethics approval

The study was performed in line with the principles of Declaration of Helsinki. Approval was granted by ethics committee of Ruijin Hospital, Shanghai Jiaotong University School of Medicine, Shanghai, People's Republic of China (04/26/2017, No. 61). Written informed consent were provided by patients before biopsy.

References

1. Wang FH, Shen L, Li J et al. (2019) The Chinese Society of Clinical Oncology (CSCO): clinical guidelines for the diagnosis and treatment of gastric cancer. Cancer Commun (Lond). 39: 10. doi: 10.1186/s40880-019-0349-9

2. Gao K, Wu J (2019) National trend of gastric cancer mortality in China (2003–2015): a population-based study. Cancer Commun (Lond). 39: 24. doi: 10.1186/s40880-019-0372-x
3. Cunningham D, Starling N, Rao S et al. (2008) Capecitabine and oxaliplatin for advanced esophagogastric cancer. N Engl J Med. 358: 36–46. doi: 10.1056/NEJMoa073149
4. Sharma P, Siddiqui BA, Anandhan S, Yadav SS, Subudhi SK, Gao J, Goswami S, Allison JP (2021) The Next Decade of Immune Checkpoint Therapy. Cancer Discov. 11: 838–57. doi: 10.1158/2159-8290.CD-20-1680
5. Kang YK, Boku N, Satoh T et al. (2017) Nivolumab in patients with advanced gastric or gastro-oesophageal junction cancer refractory to, or intolerant of, at least two previous chemotherapy regimens (ONO-4538-12, ATTRACTION-2): a randomised, double-blind, placebo-controlled, phase 3 trial. Lancet. 390: 2461–71. doi: 10.1016/S0140-6736(17)31827-5
6. Fukuoka S, Hara H, Takahashi N et al. (2020) Regorafenib Plus Nivolumab in Patients With Advanced Gastric or Colorectal Cancer: An Open-Label, Dose-Escalation, and Dose-Expansion Phase Ib Trial (REGONIVO, EPOC1603). J Clin Oncol. 38: 2053–61. doi: 10.1200/JCO.19.03296
7. Janjigian YY, Shitara K, Moehler M et al. (2021) First-line nivolumab plus chemotherapy versus chemotherapy alone for advanced gastric, gastro-oesophageal junction, and oesophageal adenocarcinoma (CheckMate 649): a randomised, open-label, phase 3 trial. Lancet. 398: 27–40. doi: 10.1016/S0140-6736(21)00797-2
8. Xu J, Jin Y, Liu Y, Zhou H, Wang Y (2019) ORIENT-16: Sintilimab plus XELOX vs placebo plus XELOX as 1st line treatment for unresectable advanced gastric and GEJ adenocarcinoma. Cancer Research. AACR Annual Meeting: Abstract CT213.
9. Kundel Y, Sternschuss M, Moore A, Perl G, Brenner B, Goldvaser H (2020) Efficacy of immune-checkpoint inhibitors in metastatic gastric or gastroesophageal junction adenocarcinoma by patient subgroups: A systematic review and meta-analysis. Cancer Med. 9: 7613–25. doi: 10.1002/cam4.3417
10. Bai R, Lv Z, Xu D, Cui J (2020) Predictive biomarkers for cancer immunotherapy with immune checkpoint inhibitors. Biomark Res. 8: 34. doi: 10.1186/s40364-020-00209-0
11. Ocana A, Nieto-Jimenez C, Pandiella A, Templeton AJ (2017) Neutrophils in cancer: prognostic role and therapeutic strategies. Mol Cancer. 16: 137. doi: 10.1186/s12943-017-0707-7
12. Valero C, Lee M, Hoen D et al. (2021) Pretreatment neutrophil-to-lymphocyte ratio and mutational burden as biomarkers of tumor response to immune checkpoint inhibitors. Nat Commun. 12: 729. doi: 10.1038/s41467-021-20935-9
13. Hanahan D (2022) Hallmarks of Cancer: New Dimensions. Cancer Discov. 12: 31–46. doi: 10.1158/2159-8290.CD-21-1059
14. Dura B, Choi JY, Zhang K, Damsky W, Thakral D, Bosenberg M, Craft J, Fan R (2019) scFTD-seq: freeze-thaw lysis based, portable approach toward highly distributed single-cell 3' mRNA profiling. Nucleic Acids Res. 47: e16. doi: 10.1093/nar/gky1173

15. Liao Y, Smyth GK, Shi W (2014) featureCounts: an efficient general purpose program for assigning sequence reads to genomic features. Bioinformatics. 30: 923–30. doi: 10.1093/bioinformatics/btt656
16. Satija R, Farrell JA, Gennert D, Schier AF, Regev A (2015) Spatial reconstruction of single-cell gene expression data. Nat Biotechnol. 33: 495–502. doi: 10.1038/nbt.3192
17. Yu G, Wang LG, Han Y, He QY (2012) clusterProfiler: an R package for comparing biological themes among gene clusters. OMICS. 16: 284–7. doi: 10.1089/omi.2011.0118
18. Zhang Y, Liu T, Hu X et al. (2021) CellCall: integrating paired ligand-receptor and transcription factor activities for cell-cell communication. Nucleic Acids Res. 49: 8520–34. doi: 10.1093/nar/gkab638
19. Sun J, Chen X, Gao P et al. (2016) Can the Neutrophil to Lymphocyte Ratio Be Used to Determine Gastric Cancer Treatment Outcomes? A Systematic Review and Meta-Analysis. Dis Markers. 2016: 7862469. doi: 10.1155/2016/7862469
20. Lalani AA, Xie W, Martini DJ et al. (2018) Change in Neutrophil-to-lymphocyte ratio (NLR) in response to immune checkpoint blockade for metastatic renal cell carcinoma. J Immunother Cancer. 6: 5. doi: 10.1186/s40425-018-0315-0
21. Capone M, Giannarelli D, Mallardo D et al. (2018) Baseline neutrophil-to-lymphocyte ratio (NLR) and derived NLR could predict overall survival in patients with advanced melanoma treated with nivolumab. J Immunother Cancer. 6: 74. doi: 10.1186/s40425-018-0383-1
22. Fukui T, Okuma Y, Nakahara Y et al. (2019) Activity of Nivolumab and Utility of Neutrophil-to-Lymphocyte Ratio as a Predictive Biomarker for Advanced Non-Small-Cell Lung Cancer: A Prospective Observational Study. Clin Lung Cancer. 20: 208 – 14 e2. doi: 10.1016/j.cllc.2018.04.021
23. Coffelt SB, Wellenstein MD, de Visser KE (2016) Neutrophils in cancer: neutral no more. Nat Rev Cancer. 16: 431–46. doi: 10.1038/nrc.2016.52
24. Mollinedo F (2019) Neutrophil Degranulation, Plasticity, and Cancer Metastasis. Trends Immunol. 40: 228 – 42. doi: 10.1016/j.it.2019.01.006
25. Mantovani A, Cassatella MA, Costantini C, Jaillon S (2011) Neutrophils in the activation and regulation of innate and adaptive immunity. Nat Rev Immunol. 11: 519–31. doi: 10.1038/nri3024
26. Wei SC, Levine JH, Cogdill AP et al. (2017) Distinct Cellular Mechanisms Underlie Anti-CTLA-4 and Anti-PD-1 Checkpoint Blockade. Cell. 170: 1120-33 e17. doi: 10.1016/j.cell.2017.07.024
27. Shergold AL, Millar R, Nibbs RJB (2019) Understanding and overcoming the resistance of cancer to PD-1/PD-L1 blockade. Pharmacol Res. 145: 104258. doi: 10.1016/j.phrs.2019.104258
28. Mayoux M, Roller A, Pulko V et al. (2020) Dendritic cells dictate responses to PD-L1 blockade cancer immunotherapy. Sci Transl Med. 12. doi: 10.1126/scitranslmed.aav7431
29. Camelliti S, Le Noci V, Bianchi F et al. (2020) Mechanisms of hyperprogressive disease after immune checkpoint inhibitor therapy: what we (don't) know. J Exp Clin Cancer Res. 39: 236. doi: 10.1186/s13046-020-01721-9

30. Arasanz H, Zuazo M, Bocanegra A et al. (2021) Hyperprogressive Disease: Main Features and Key Controversies. Int J Mol Sci. 22. doi: 10.3390/ijms22073736
31. Catenacci DVT, Tebbutt NC, Davidenko I et al. (2017) Rilotumumab plus epirubicin, cisplatin, and capecitabine as first-line therapy in advanced MET-positive gastric or gastro-oesophageal junction cancer (RILOMET-1): a randomised, double-blind, placebo-controlled, phase 3 trial. Lancet Oncol. 18: 1467–82. doi: 10.1016/S1470-2045(17)30566-1
32. Anestis A, Zoi I, Karamouzis MV (2018) Current advances of targeting HGF/c-Met pathway in gastric cancer. Ann Transl Med. 6: 247. doi: 10.21037/atm.2018.04.42
33. Yu Z, Li Z, Wang C et al. (2019) Oncostatin M receptor, positively regulated by SP1, promotes gastric cancer growth and metastasis upon treatment with Oncostatin M. Gastric Cancer. 22: 955–66. doi: 10.1007/s10120-019-00934-y
34. Dahan R, Sega E, Engelhardt J, Selby M, Korman AJ, Ravetch JV (2015) FcgammaRs Modulate the Anti-tumor Activity of Antibodies Targeting the PD-1/PD-L1 Axis. Cancer Cell. 28: 285–95. doi: 10.1016/j.ccell.2015.08.004
35. Arlauckas SP, Garris CS, Kohler RH et al. (2017) In vivo imaging reveals a tumor-associated macrophage-mediated resistance pathway in anti-PD-1 therapy. Sci Transl Med. 9. doi: 10.1126/scitranslmed.aal3604
36. Lo Russo G, Moro M, Sommariva M et al. (2019) Antibody-Fc/FcR Interaction on Macrophages as a Mechanism for Hyperprogressive Disease in Non-small Cell Lung Cancer Subsequent to PD-1/PD-L1 Blockade. Clin Cancer Res. 25: 989–99. doi: 10.1158/1078-0432.CCR-18-1390
37. Bournazos S, Ravetch JV (2015) Fcgamma receptor pathways during active and passive immunization. Immunol Rev. 268: 88–103. doi: 10.1111/imr.12343

Tables

Table1 Clinical pathological characteristics of gastric cancer

Clinicopathological characteristics		N	percentage
Gender	Male	46	67.6%
	Female	22	32.4%
Age	Median	65	/
	Range	27-85	/
Metastatic organs	1	45	66.2%
	2	15	22.1%
	≥3	8	11.7%
Pervious lines of treatment	0	15	22.1%
	1	20	29.4%
	2	33	48.5%
Combination strategies	Monotherapy	7	10.3%
	Chemotherapy	28	41.2%
	Targeted therapy	33	48.5%
Cycles	Median	5	/
	Range	2-26	/

Figures

Figure 1

Correlation between NLR and treatment efficacy of PD-1 antibody-based therapy in advanced gastric cancer.

A: NLR-AE1 and patients' objective response; B: NLR-2C and patients' objective response; C: NLR-BL and patients' objective response; D: Patients with high NLR-2C had poorer PFS comparing with those with low NLR-2C; E: Patients with high NLR-AE1 had poorer PFS comparing with those with low NLR-AE1.

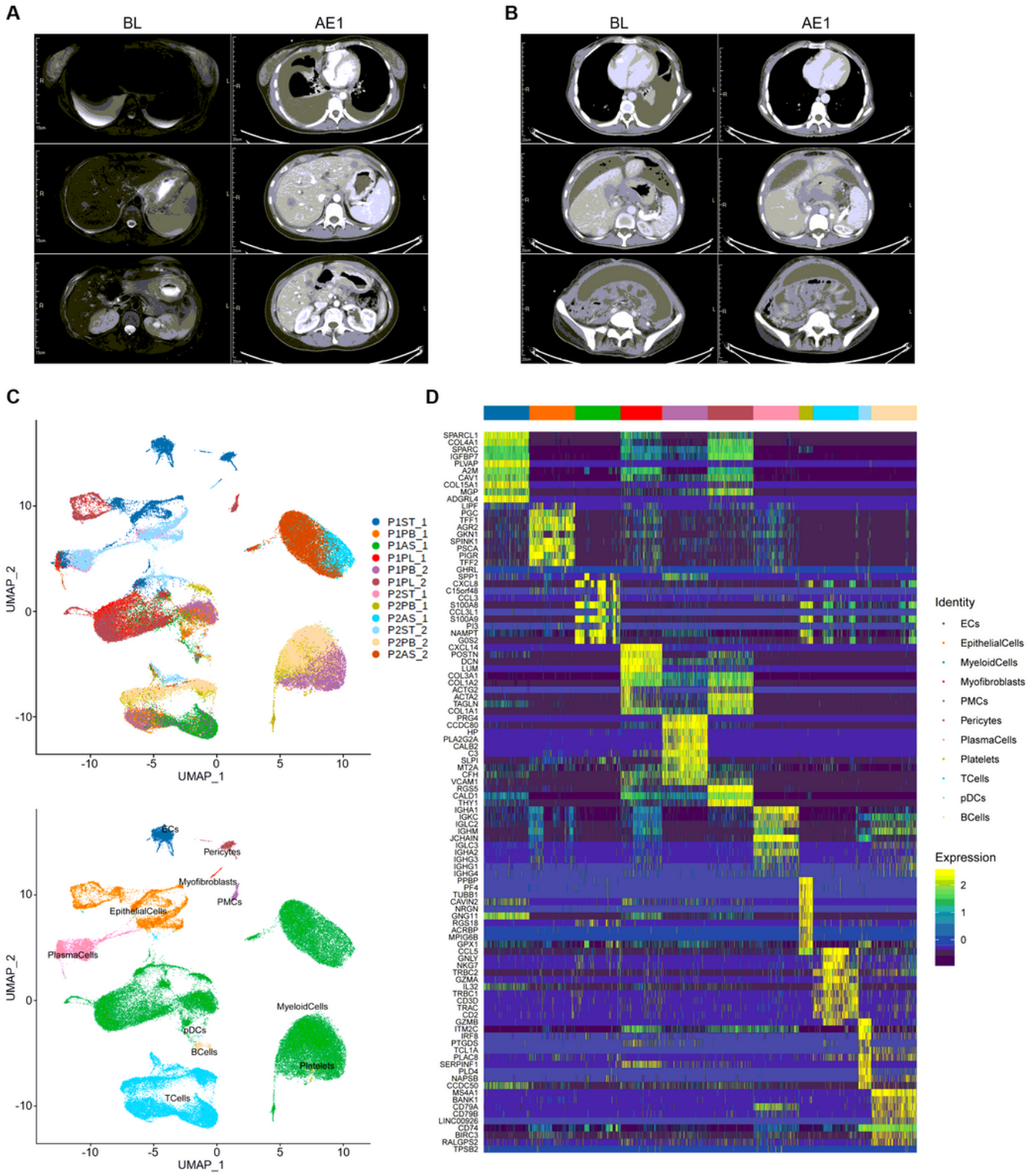

Figure 2

Clinical imaging of two AGC patients and landscape of cellular constitution of samples.

A: Pre- and posttreatment CT scan of patient 1 (P1); B Pre- and posttreatment CT scan of patient 2 (P2); C: The UMAP plot of main cell types in all 12 samples; D: Heatmap of expression of marker genes in 11 cell types.

Figure 3

Cellular constitution of immune cells in peripheral blood samples and cellular subcluster analysis of neutrophil.

A: Cellular constitution of immune cells and myeloid cells in peripheral blood samples; B: Cellular subcluster of neutrophil in peripheral blood and ascites samples; C: Dot plot of GO analysis of high expression DEGs of neutrophil cluster1 (NE-C1); D: Net plot of GO analysis of high expression DEGs of NE-C1.

Figure 4

Cellular subcluster analysis of malignant epithelial cells.

A: Copy-number variation (CNV) analysis to identified malignant epithelial cells. B: Cellular subcluster of malignant epithelial cells in primary lesion and pleural fluid samples. C: Dot plot of GO analysis of high expression DEGs of malignant epithelial cell cluster4 (EP-C4); D: Dot plot of KEGG analysis of high expression DEGs of EP-C4.

Figure 5

Cellular subcluster analysis of macrophages

A: Cellular constitution of macrophages in primary lesion and pleuroperitoneal fluids samples; B: Cellular subcluster of M2 macrophages; C: Dot plot of GO analysis of high expression DEGs of M2 macrophage cluster1 (MF-C1); D: Dot plot of GO analysis of high expression DEGs of MF-C2.

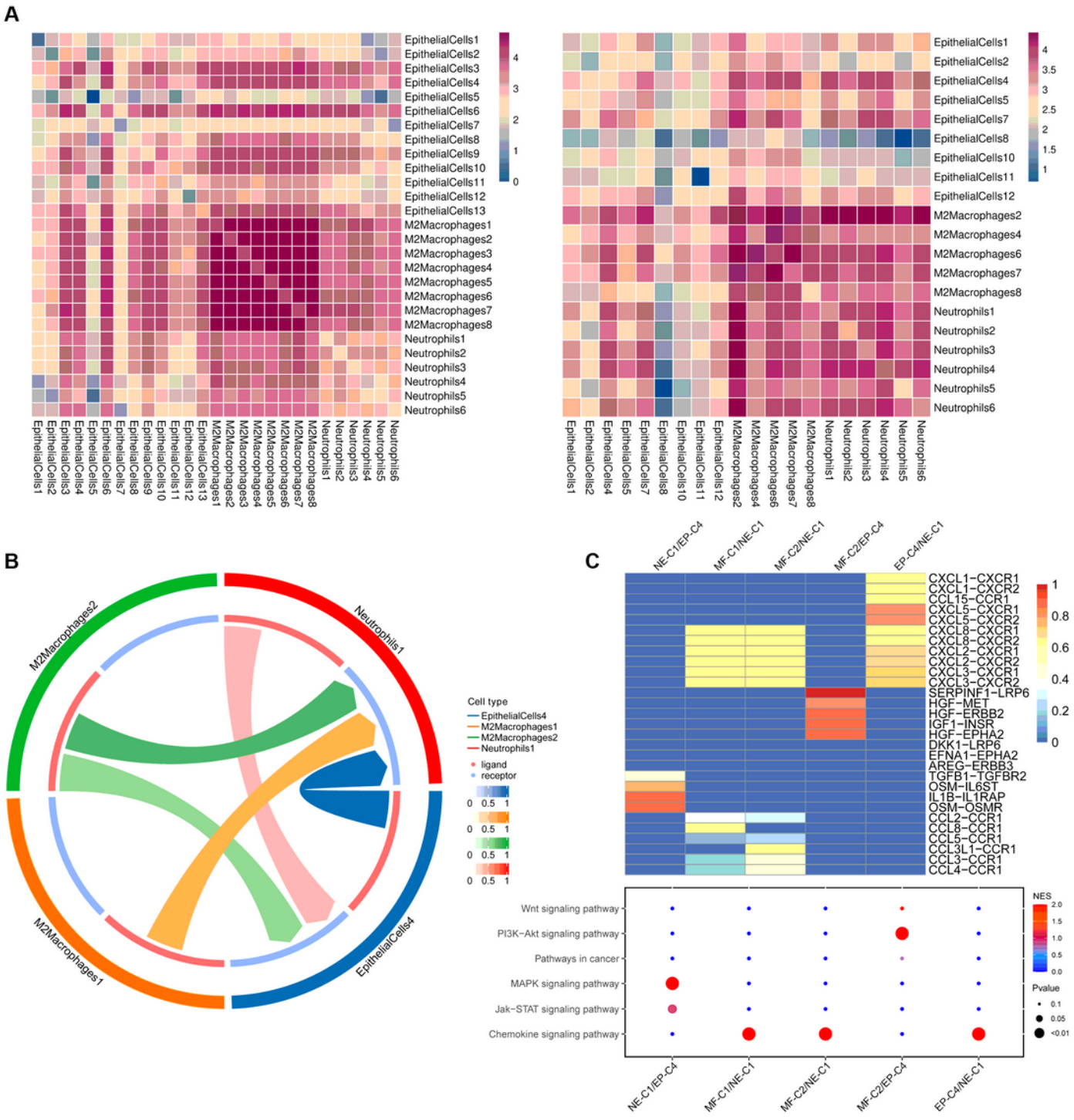

Figure 6

Cellular interaction analysis among neutrophil, malignant epithelial cell and M2 macrophage.

A: Heatmap of number of paired ligands and receptors among subclusters of neutrophil, malignant epithelial cell and M2 macrophage. B: Cell network of NE-C1, EP-C4, MF-C1 and MF-C4 was analyzed by CellCall; C: Heatmap of ligand-receptor interaction among NE-C1, EP-C4, MF-C1 and MF-C4, and ligand-receptor interactions were enriched by KEGG analysis.

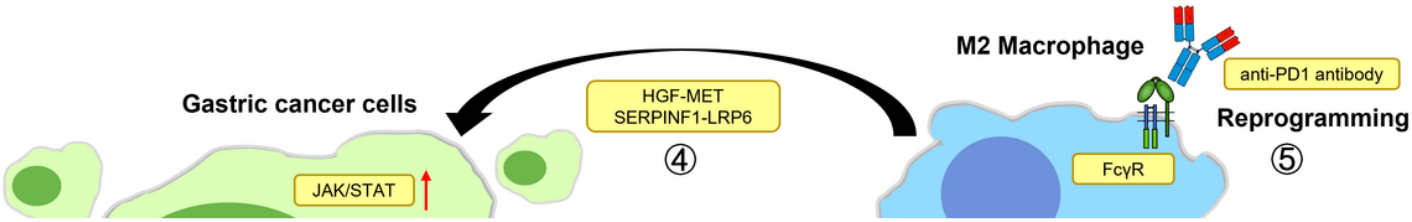

Figure 7

Underlying mechanisms of neutrophil in promoting tumor progression during PD-1 antibodies treatment

 A sub-cluster of highly activated neutrophils were identified before and after PD-1 treatment, which highly expressed tumor-promoting genes including *MMP9*, *S100A8*, *S100A9*, *PORK2*, and TGF-β1

 Activated neutrophils could promote progression of cancer cells by producing reactive oxygen species, cytokines, proteinases, and angiogenesis factors and by activating the JAK-STAT, MAPK, and PI3K signaling pathways

 Cancer cells could recruit and activate neutrophils by secreting chemokines and cytokines into the tumor microenvironment

 The ligand-receptor heat-map identified HGF as the major ligand of M2 macrophages, which could be involved in promoting gastric cancer progression

 It is inferred that PD-1-negative tumor-associated macrophages could capture PD-1 antibody with its Fcγ receptor to impair the anti-tumor activity of PD-1 antibody through reprogramming based on our findings and literatures

Supplementary Files

This is a list of supplementary files associated with this preprint. Click to download.

- FigS1.pdf
- FigS2.pdf
- TableS1.xls
- TableS2.xls
- TableS3.xls
- TableS4.xls
- TableS5.xls
- TableS6.xls
- TableS7.xls
- TableS8.xls
- TableS9.xls